Austin Journal of Clinical Ophthalmology

Open Access

Austin Publishing Group

Research Article

Energy Storage and Dissipation in the Eye: The Importance of the Biomechanical Connections between the Cornea-Limbus-Scleral Series Biomechanical Element and the Scleral-Optic Nerve-Posterior Segment Tissues in Protecting Sensitive Visual Components from Mechanical Damage

Frederick H Silver[1,2*]; Tanmay Deshmukh[2]; Dominick Benedetto[3]; Michael Gonzalez-Mercedes[2]; Jose Pulido[4]

[1]Department of Pathology and Laboratory Medicine, Robert Wood Johnson Medical School, Rutgers, the State University of New Jersey, USA

[2]OptoVibronex, LLC., Ben Franklin Tech Partners, Bethlehem, USA

[3]Center For Advanced Eye Care, Vero Beach, USA

[4]Vickie and Jack Farber Vision Research Center, Wills Eye Hospital, Philadelphia, USA

***Corresponding author: Frederick H Silver**
Department of Pathology and Laboratory Medicine, Robert Wood Johnson Medical School, Rutgers, the State University of New Jersey, USA.
Email: silverfr@rutgers.edu

Received: July 18, 2023
Accepted: August 28, 2023
Published: September 04, 2023

Abstract

An understanding of ocular biomechanics is essential to appreciate the molecular structure of the anterior and posterior segments of the eye and their role in maintaning corneal shape, refractive power and visual acuity. Energy storage, transmission and dissipation are essential elements of normal mechanical homeostasis. Vibrational Optical Coherence Tomography (VOCT) was used to study the viscoelasticity of the anterior and posterior segments of the porcine eye. Our VOCT results indicate that both the cornea and retina are highly viscoelastic tissues that can dissipate large amounts of applied energy to support mechanical homeostasis of the anterior and posterior segments of the eye. We conclude that a relationship exists between the anterior cornea-limbus-scleral series biomechanical unit and the posterior sclera-retina complex that assists in energy dissipation. This relationship limits structural changes in the eye and supports delicate ocular posterior segment structures like the retina and optic nerve from acute or chronic insult

Keywords: Cornea; Sclera; Limbus; Retina; Optic nerve; Bruch's membrane; Choroid; Lamina cribrosa; Viscoelasticity; Loss modulus; Elastic modulus; Stiffness; Collagen

Introduction

Energy storage, transmission and dissipation are important functions that prevent cornea delamination and mechanical damage to the visual components in the posterior segment of the eye [1]. Significant scleral thinning and tissue loss, particularly at the posterior pole of the eye, has been associated with ocular enlargement and myopia development [2] while the shape of the posterior sclera has been viewed as a sign of open-angle glaucoma [3]. Scleral thinning may be due to tensile stretching and creep of the sclera as a result of external and internal forces that act on the cornea-limbus-scleral biomechanical unit [1].

On earth, all ocular tissues experience gravitational forces that exceed 760 mm Hg. Gravitational and other external forces must be offset by internal forces within the eye, or the entire globe would deflate. The loss of gravity has been reported to cause the globes of astronauts to flatten and the optic nerve length to change, resulting in modification of the location of the optic nerve head [4,5]. In addition to gravity, the cornea experiences several other forces including shearing, lid pressure, surface tension associated with the tear film, extraocular muscle stress, intraocular pressure, and tension in the cornea due to internal stretching [1]. In dermal tissue the balance between internal and external stresses has been reported to modulate mechanotransduction and the balance between tissue atrophy and tissue deposition [6]. Blunt external forces acting on the cornea cause corneal deformation. The cornea must store and then transmit this energy to the anterior and posterior segments of the eye to prevent corneal delamination and tearing. If this energy is not dissipated, mechanical fatigue and struc-

Citation: Silver FH, Deshmukh T, Benedetto D, Gonzalez-Mercedes M, Pulido J. Energy Storage and Dissipation in the Eye: The Importance of the Biomechanical Connections between the Cornea-Limbus-Scleral Series Biomechanical Element and the Scleral-Optic Nerve-Posterior Segment Tissues in Protecting Sensitive Visual Components from Mechanical Damage. Austin J Clin Ophthalmol. 2023; 10(6): 1162.

tural failure of both anterior and sensitive posterior segment structures like the retina and optic nerve may result. Since the cornea does not delaminate during blunt trauma, this energy must be transmitted to other parts of the eye where it is dissipated. It has been proposed that this energy is transmitted through the attachments of the cornea and limbus to the posterior sclera [1]. It is important to understand how and where this energy is dissipated in the eye since any anatomic changes that occur to the posterior scleral connection to the optic nerve could lead to a loss of visual acuity.

While energy storage, transmission and dissipation have been addressed in tissues including skin, tendon, muscle, blood vessels and cartilage [6-12], very little attention has been paid to how energy is stored, transmitted, and dissipated in the eye. While the cornea is the major tissue that protects the visual components in the anterior and posterior segments of the eye from mechanical damage, it is in series mechanically with the limbus and sclera [1]. Recently it was pointed out that the corneal-limbus-scleral biomechanical unit and the integration of the circumferential and collagen fibrillar networks in the cornea are important in preventing corneal delamination [1]. This mechanism of energy dissipation was further hypothesized to protect the cornea from changes in shape, curvature, and therefore, refractive power. Ultimately, energy dissipation of both external and internal forces acting on the globe and the mechanical connection between the anterior and posterior segments may lead to thinning of the sclera and be associated with several ocular diseases [13].

Energy storage, transmission and dissipation by mammalian tissues has been elucidated by x-ray diffraction and biomechanical studies on both tendon, skin and cartilage [14-18]. These properties are a consequence of the viscoelasticity of the macromolecular components found in extracellular matrices [19]. They are related to the ability of extracellular matrices to undergo reversible stretching of the collagen triple helix (energy storage), reversible stretching of collagen molecules and cross-links, and sliding of the quarter-staggered collagen molecules [14-18]. These deformation mechanisms increase the D period (energy storage and transmission), and result in energy dissipation through sliding and rearrangement of both water and proteoglycans surrounding collagen fibrils [14-20].

Previous pilot studies on both human and porcine eyes indicate that they have similar mechanovibrational peaks and moduli; however they do differ in the resonant frequency peak amplitudes at 80, 120, 150 and 250 Hz [1,21]. The resonant frequencies of cellular, fibrillar collagen, blood vessels, and fibrotic collagen are related to their elastic moduli (stiffness) [1] and changes in resonant frequency and modulus may be used as markers of skin and other tissue pathologies [22,23]. While It is known that the stroma of porcine cornea is much thicker than that of human corneas, the porcine eye has been used as a good model of the anatomy and mechanical behavior of the human eye. The similarity between the resonant frequency peaks near 80, 120, 150 and 250 Hz of human and porcine corneas, sclera and limbus, suggest that the anatomically described layers in these tissues are connected in a single biomechanical unit that can store external mechanical energy with transmission to the posterior segment of the eye for dissipation [1].

In this publication, we compare the viscoelasticity of both the anterior and posterior segments of porcine eyes in order to determine which parts of the eye are able to dissipate large amounts of energy as a result of external and internal mechanical loading. In addition, the resonant frequency and elastic modulus of excised components of porcine eyes are measured to further characterize the biomechanical properties of individual components of the eye.

Materials and Methods

Resonant Frequency and Elastic Modulus Measurements

Vibrational Optical Coherence Tomography (VOCT) is a technique that uses infrared light that is reflected to a detector from different depths in a tissue to create an image. By applying an acoustic force and measuring the change in displacement of the tissue components, it is possible to calculate the component tissue stiffnesses [1,20-23]. The experimental setup for VOCT is shown in Figure 1. A stiffer component will have a larger displacement than a softer component under a fixed load. The weighted displacement of a tissue is obtained after correction for the displacement of the speaker, background noise, and out-of-phase vibrations (viscoelasticity) as a function of frequency to isolate the elastic response. The normalized weighted displacement is a unitless number and is the ratio of the displacement of the sample divided by the displacement in the absence of the sample. Mechanovibrational VOCT spectra were collected on porcine whole globes and excised components of the porcine eyes in vitro. 30 fresh porcine eyes were obtained from Spear products (Coopersburg, PA USA) and kept on ice during transport for testing. The pigs weighed 220 to 280 lbs. and were 6 to 12 months old. Porcine eyes were studied using VOCT within 4 hours of harvesting at Ben Franklin Tech Ventures (Bethlehem, PA, USA). It was noted that the excised corneal thickness increased after excision even when kept on ice. The porcine eyes were studied intact after removal of the extraocular muscles and conjunctiva, as well as after the cornea, and parts of the cornea and posterior segment were removed by dissection.

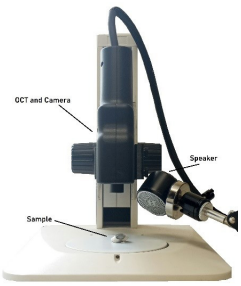

Figure 1: Photograph of setup for measuring the frequency dependence of the weighted displacement using Vibrational Optical Coherence Tomography (VOCT). The speaker, OCT handpiece that is connect to an I5 computer embedded in the OCT engine (camera), and the microscope stand on which the excised cornea is placed is shown.

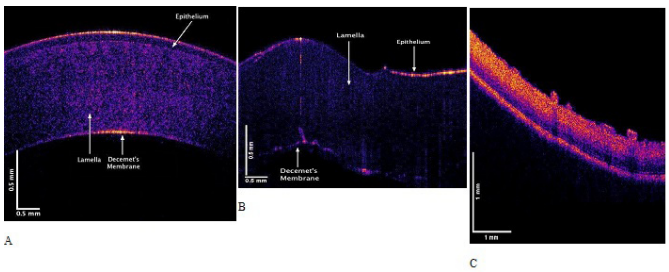

Figure 2: Color-coded OCT images of porcine cornea in an intact globe in vitro (A), and an excised porcine cornea in vitro (B). Note the porcine cornea is thicker than that of the human. When the tension is released after it is excised the porcine cornea folds. (C) OCT image of the posterior segment of the porcine eye showing retina.

OCT Images

OCT image collection was conducted using a Lumedica Spectral Domain OQ 2.0 Labscope (Lumedica Inc., Durham, NC, USA) operating in the scanning mode at a wavelength of 840 nm. The device generates a 512x512-pixel image with a transverse resolution of 15 micrometers and an A-scan rate of 13,000/sec. All gray scale OCT images were color-coded based on the pixel intensity to enhance the image details. The images were used to locate exactly where the VOCT measurements were made on each sample. This device was modified by adding a speaker that generated an acoustic signal and special software capable of analyzing OCT raw images for VOCT measurements.

Resonant Frequency and Elastic Modulus

The OQ Labscope was modified by adding a speaker 2 inches in diameter (A106 Pro, JYM Electronics Co., Ltd, Shajing Town, China) to vibrate the tissue at 55dB sound pressure density in the VOCT studies [1,20-23]. The Labscope was also modified to collect and store single unprocessed raw OCT image data that was used to calculate sample displacements (amplitude information) from amplitude line data. The data was processed using MATLAB software R2020a version 9.8 (Mathworks, Natick MA, USA) as discussed previously [20-23]. The displacement of the tissue was detected by measuring the frequency dependence of the deformation based on the reflected infrared light. The light was filtered to collect only vibrations that were in phase (elastic component) with the sound input. The vibrations for each frequency were collected and stored on the cloud for further analysis as a mechanovibrational spectrum. The mechanovibrational spectral peaks were normalized by dividing by the largest peak in each spectrum to correct for speaker orientation and varying sound levels that occur during data collection on different samples.

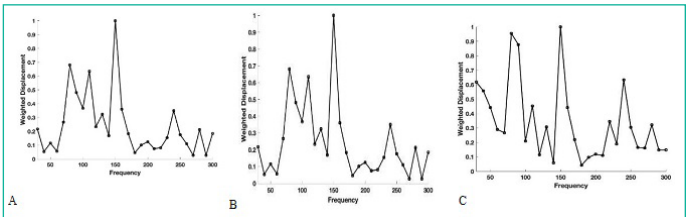

Figure 3: Typical plots of weighted displacement versus frequency for porcine cornea in an intact globe in vitro (A), and isolated excised porcine cornea in vitro (B). Both human and porcine corneas contain peaks at 80 to 90 Hz, 100 to 120 Hz, 150 to 160 Hz and 240 to 250 Hz [1,20]. (C) Weighted displacement versus frequency for the retina and posterior segiment of a porcine eye.

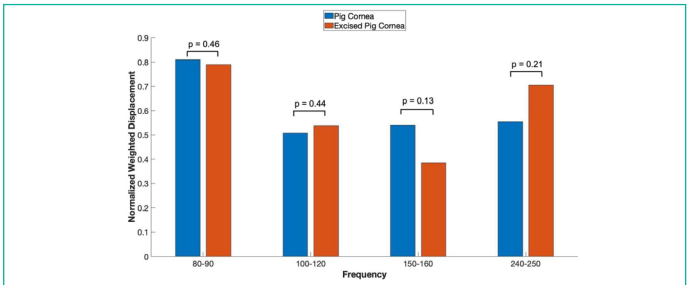

Figure 4: Normalized weighted displacement versus frequency plots of porcine whole globe and excised porcine cornea in vitro. Weighted displacement versus frequency peaks were normalized by dividing by the largest peak in each spectrum. Normalization was made to correct for differences in speaker orientation and the speaker distance away from the eye when the measurements are made. P values are shown above the bars for comparison of the data for different samples. Note no significant differences were observed between measurements made on whole globes and excised corneas. N for pig corneas = 18, and N for excised cornea = 7.

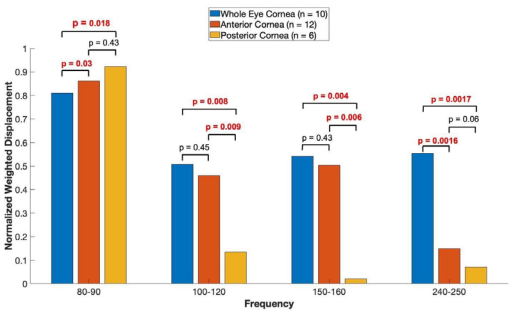

Figure 5: Shows a plot of normalized average weighted displacement versus frequency, for whole pig cornea, excised portions of the anterior porcine cornea, and excised portions of the retina and posterior porcine cornea measured in vitro. Weighted displacement versus frequency peaks were normalized by dividing by the largest peak in each spectrum. Normalization was made to correct for differences in speaker orientation and the speaker distance away from the eye when the measurements were made. The 80 to 90 Hz peak appears to have an origin in the anterior and posterior cornea, the 100 to 120 Hz and the 150 to 160 Hz peaks appear to originate in the anterior portion of the cornea. The 240-250 Hz peak appears to originate from the whole eye as opposed to only the cornea. The sample sizes studied are shown in the image.

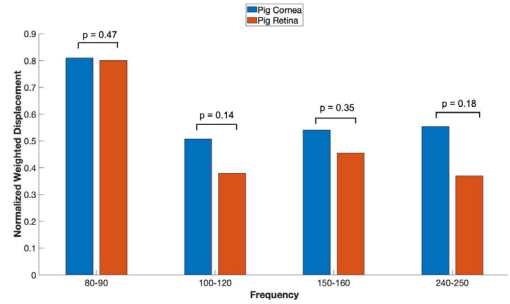

Figure 6: shows VOCT normalized average weighted displacement with the OCT focused on porcine cornea versus the OCT focused on the excised porcine retina containing the retina and all other components of the posterior segment in vitro. Normalization was made to correct for differences in speaker orientation and the speaker distance away from the eye when the measurements were made. Note all the peaks are found in the anterior and posterior segments of porcine eyes. N=18 for pig cornea and N=8 for pig retina.

The resonant frequency of a tissue component is defined as the frequency at which the maximum in-phase displacement (maximum energy storage) is observed in the amplitude data. The measured resonant frequencies are converted into elastic modulus values using an empirical calibration equation (Eqn. 1) developed based on *in vitro* uniaxial mechanical tensile testing and VOCT measurements made on the same tissue at the same time as reported previously [1,20-23]. The resonant frequency of tissue components in vitro and in vivo such as cells, blood vessels, collagen fibers and fibrous tissue are similar in different soft tissues [20-23]. The resonant frequency of each sample is determined by measuring the transverse displacement of the tissue resulting from applied sinusoidal audible sound driving frequencies ranging from 30 Hz to 300 Hz, in steps of 10 Hz. Since the measurements were made at 10 Hz steps the resonant frequencies were observed to occur at intervals of +/- 10 Hz. For this reason, the location of the peaks on some of the samples differ by as much as 10 Hz. The peak frequency (the resonant frequency), f_n, is defined as the frequency at which the displacement is maximized after the vibrations due to the speaker are removed.

$$E = \frac{0.0651\ x\ (fn^2) + 233.16}{d} \qquad (1)$$

Since soft tissues have a density very close to 1.0; equation (1) is valid for most tissues found in the body as well as for several synthetic polymers; where the thickness d is in m and is determined from OCT images, fn^2 is the square of the resonant frequency, and E is the tensile elastic modulus in MPa as discussed previously [1]. Equation (1) was used to calculate the modulus values and is an empirical equation based on calibration studies using decellularized human skin (dermal collagen), animal tissues, and synthetic polymers tested in uniaxial tension and simultaneously using VOCT [1,20-23]. The elastic modulus measured using VOCT is a materials property at the resonant frequency at low strains since the viscous component of the behavior is only 5% to 7% at frequencies above 110 Hz of the total modulus [18,19] and the modulus is unchanged at strains less than about 7% for collagenous materials [18,19].

Loss Modulus Measurements

The viscous component of the modulus is estimated as a fraction of the total modulus (elastic plus viscous components) captured at each frequency studied. To achieve this, the specimen undergoes a variation of the VOCT protocol that was used to measure the resonant frequency. The specimen is subjected to three pulses of audible sound at known frequencies from 30 to 300 in steps of 10 Hz. The sample vibrational spectrum is then collected after the vibrations are terminated, and the peak heights and widths are analyzed as a function of frequency. The viscous component is obtained by dividing the change in frequency at the half height of the mechanovibrational peak, or 3 decibels down from the maximum peak in the power spectrum, by the driving frequency. This method is known as the half-height bandwidth method [20]. The width of the displacement peak in this test is related to the time dependence of the viscoelastic response and the loss modulus. The loss modulus increases proportionally to the time required for the material to return to its original thickness after the sound is removed.

Statistics

All resonant frequencies were analyzed for statistical differences using an upaired one-tailed unpaired Student's t test and the differences were considered significant if the p value was less than 0.05.

Results

Figure 2 shows OCT images of porcine cornea in a whole globe in vitro (A) and an excised porcine cornea in vitro (B). Note the human cornea is much thinner than the porcine cornea in the entact globe. When the porcine cornea is excised from the porcine globe it folds (B) as a result of the loss of the internal corneal tension that pulls the cornea tightly over the entire globe. The cornea appears to be stretched in tension over the surface of the globe even in the absence of extraocular muscle tension; this tension transmits applied forces through the limbus to the posterior sclera. Figure 2C shows a color-coded OCT image of the retina and posterior segment.

Figure 3 shows plots of weighted displacement versus frequency for porcine cornea with an intact globe (A), isolated excised porcine cornea (B) and (C) the porcine retina and posterior segment. Both human and porcine corneas contain peaks at 80 to 90 Hz, 100 to 120 Hz, 150 to 160 Hz and 240 to 250 Hz as previously reported [1,2]. These peaks are still present in the excised porcine cornea and characterize different parts of the cornea in the cornea-limbus-sclera biomechanical unit as discussed previously [1].

Figure 4 shows bar graphs comparing the normalized weighted displacement versus frequency plots for porcine cornea when the measurements were made on the whole globe focused on cornea and excised porcine cornea. Note the only significant difference in the peak heights observed was in the 80 to 90 Hz peak reflecting the increased thickness and cellularity of the porcine cornea. P values are shown above the bars for comparison of the data for different samples. The are no statistical differences between the resonant frequency peaks of the whole globes and excised corneas.

A plot of normalized average weighted displacement versus frequency for whole porcine globe, excised portions of the anterior porcine cornea, and excised portions of the retina and posterior porcine cornea in vitro are shown in Figure 5. The 80 to 90 Hz peak appears to have an origin in the anterior and posterior portions of the cornea, the 100 to 120 Hz and the 150 to 160 Hz peaks appear to originate in the anterior portion of the cornea. The 240-250 Hz peak appears to be found in the whole eye and may be from the corneal-limbus interface.

When in vitro VOCT measurements were made comparing the OCT focused on the cornea versus the OCT focused on the retina (retina, optic nerve and more posterior tissues left intact), the mechanovibrational peaks are seen to be similar. Figure 6 shows normalized average weighted displacement versus frequency plots exhibit no differences in any of the peaks. These peaks appear to originate in both the cornea and the anterior segment of the cornea.

Figure 7 shows a plot of loss modulus as a fraction of the elastic modulus versus frequency for whole porcine globe focused on the cornea and isolated cornea in vitro. Note the loss modulus decreases with increasing frequency and is similar in porcine globes and excised corneas. At low mechanical loading frequency, the cornea is highly viscoelastic and mechanical measurements made at frequencies below 150 Hz need to be corrected for frequency and strain-rate dependence of the data.

When the loss modulus versus frequency is compared for infrared light focused on the porcine cornea and that focused on the porcine retina and posterior segment after the cornea and lens are removed, a trend similar to Figure 7 is observed. Both porcine cornea and porcine retina and posterior segment

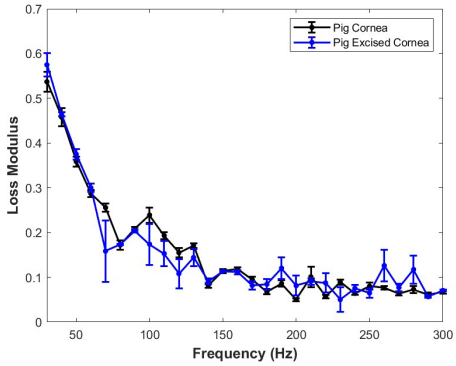

Figure 7: A plot of loss modulus as a fraction of the elastic modulus versus frequency for whole pig globe focused on the cornea versus excised cornea in vitro. These measurements were conducted after pulsing the sample with acoustic sound and then making measurements directly after removing the acoustic signal. Note the loss modulus decreases with increasing frequency and is similar in pig globes and excised corneas. At low mechanical loading frequency, the cornea is highly viscoelastic and mechanical measurements made at frequencies below 150 Hz need to be corrected for frequency and strain-rate dependence. N=18 for pig cornea and N=7 for pig excised cornea.

appear to be highly viscoelastic with the cornea and posterior segment having similar viscoelasticity (Figure 8).

A plot of loss modulus versus frequency for infrared light focused on the isolated porcine retina after the cornea and lens are removed is shown in Figure 7. Both cornea and pig retina components are highly viscoelastic. The high viscoelasticity of isolated porcine retina components including the optic nerve and sheath, indicates that the retina, optic nerve, sheath, and posterior segment tissues all possess energy dissipating abilities. These results indicate that both anterior and posterior segment tissues dissipate large amounts of external and internal mechanical energy applied to the eye. This is accomplished without structural changes to the anterior and posterior segments of the eye. The dissipation energy by anterior and posterior segment eye components may involve transfer of excess energy through mechanical vibrations to the aqueous and vitreous humor as well as to other components of the anterior and posterior chambers.

These observations suggest that the tensile or Young's modulus measured on ocular tissues at low frequencies must be corrected to properly determine the elastic modulus of ocular tissues.

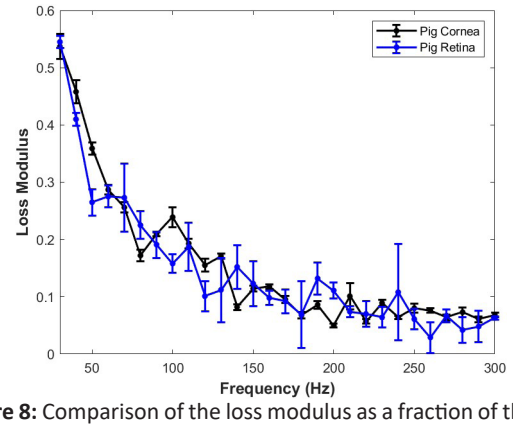

Figure 8: Comparison of the loss modulus as a fraction of the elastic modulus versus frequency for infrared light focused on porcine cornea and that focused on the porcine retina and posterior segment after the cornea and lens are removed in vitro. Both cornea and retina and posterior segment appear to have similar viscoelastic properties. The loss modulus approaches that of the elastic modulus at high frequencies. This data suggests that both cornea and posterior segment components of the porcine eye are highly viscoelastic and can store and dissipate large amounts of mechanical energy. N=18 for pig cornea and N=8 for pig retina.

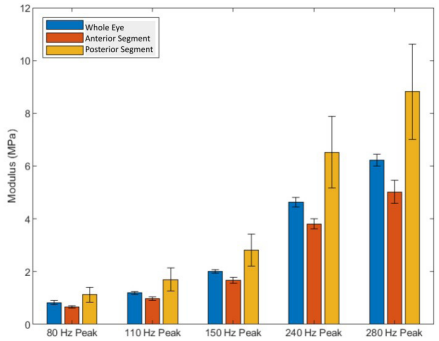

Figure 9: Bar plot comparison of the tensile elastic moduli for standard deviations for whole eye focused on the cornea, excised cornea (anterior segment) and light focused on the retina (posterior segment). The values listed for the cornea include vibrations from the limbus while those from the retina reflect contributions from the optic nerve, lamina crobosa, choroid and poesterior sclera. The peaks listed are at 80, 110, 150, 240 and 280 Hz. N=10 whole eye, N=12 excised cornea, and N=6 retina and posterior segment.

Figure 9 lists the tensile elastic moduli and standard deviations for the moduli of the whole eye focused on the cornea, excised cornea (anterior segment) and that focused on the retina (posterior segment)

Discussion

The results reported in this paper suggest that the anterior and posterior segments of the eye contain highly viscoelastic tissues that prevent mechanical damage to the eye by storing, transmiting and dissipating energy at low frequencies. The anterior and posterior segments of the eye are thought to be linked both structurally and functionally through the corneal-limbus-scleral connection [13]. In this study, we demonstrate that viscous losses and energy dissipation in the cornea are similar to that seen in the retina and posterior segment of the eye. This suggests that one of the the cornea's physiological roles is to dissipate applied energy and then transfer it away from the cornea to be dissipated elsewhere in the posterior segment of the eye. The cornea stores, transmits and dissipates energy applied by external and internal forces maintaining the structure, shape, and curvature of the cornea and maintaining visual acuity. Ultimately, forces applied to the eye, must be dissipated somewhere in the eye or they will eventually lead to changes in the structure and properties of delicate components in the posterior ocular segment.

Energy stored in the anterior segment of the eye is likely to be dissipated not only by stretching the limbus-scleral junction, but also by increasing intraocular pressure, inducing aqueous humor outflow and increasing deformation of the trabecular meshwork similar to how energy dissipation occurs in blood vessels [12]. In blood vessels, increased blood pressure and kinetic energy is transferred to the vessel wall by increasing the vascular diameter and via longitudinal stretching as the pulse wave travels down the vascular tree [12]. Analogous to what happens in blood vessels, pressure applied to the cornea is not only transferred to the posterior cornea, but it will induce pressure in the anterior chamber that ultimately is transferred to the trabecular meshwork. In contrast in the posterior segment, viscous dissipation is likely to occur by deformation of the retina and vitreous humor, which is a highly swollen network of collagen and proteoglycans. At low impact frequencies vitreous humor deformation can dampen forces and dissipate energy transmitted posteriorly to the optic nerve similar to how a shock absorber displaces a viscous fluid with a piston. In contrast, at high impact frequencies it is likely that energy is transmitted from the anterior chamber to the vitreous and then passed to the retina, Bruch's membrane, choroid and sclera. High impact energy can cause tearing of Bruch's membrane, choroid and sclera. Any changes in the mechanical properties of the cornea, sclera, lamina cribosa, and associated posterior segment tissues can down or upregulate mechanotranduction leading to either new tissue deposition or tissue atrophy.

Mechanical cycling of the macromolecular components of the anterior and posterior segments of the eye occur as a result of changes in gravitational forces (standing versus laying down), or during changes in extraocular and intraocular muscular forces associated with accommodation when reading. Other factors that may affect mechanical loading of the eye include changes in scleral stiffness [23], ocular pulse amplitude and decreased pulse volume [24], increased cerebral spinal fluid pressure, and the optic nerve tissue pressure that are part of the trans-lamina cribrosa pressure gradient [25].

Ocular tissues undergo millions of cycles of applied forces due to changes in the gravitational force vector, changes in barometric pressure, ocular arterial and Cerebrospinal (CSF) pulse pressures or accommodation. This could cause changes in the structure and composition of both the anterior and posterior segments of the eye. Changes in the mechanical equilibrium between the cornea-limbus-sclera biomechanical unit and the sclera-optic nerve retina posterior complex could alter cellular division, protein synthesis and catabolism that could eventually lead to ocular diseases such as myopia and glaucoma. Early changes that are associated with these diseases may be detected and monitored by measuring changes in the viscoelastic properties of anterior and posterior segment structural components. Overloading of these structural components could cause tisssue atrophy and structural changes to the trabecular meshwork, sclera, optic nerve and other posterior components of the eye.

The posterior segment of the eye contains connections between the sclera, optic nerve, lamna cribosa, choroid, Bruch's membrane and retina. Stretching or thinning of the posterior sclera [26] would also affect the optic nerve and lamina cribosa which in turn would lead to forces being applied to the retina and Bruch's membrane. Any energy transferred to the back of the eye through the cornea-limbus-sclera biomechanical unit must be dissipated somewhere posteriorly in order to prevent changes in the optic nerve and retina that could ultimately affect visual acuity.

Recently, several major ophthalmic conditions have been linked to corneal and scleral biomechanical properties, such as ametropia, corneal pathologies, ocular surface disease, and glaucoma [2]. It has been demonstrated that scleral thinning and biomechanical changes are linked to a general loss of collagen and proteoglycans in regions of the posterior sclera. [27,28]. In the early stage of myopia development, new collagen production is reduced rapidly, mostly of type I collagen, which accounts for approximately 99% of scleral collagen. Existing collagen degradation occurs in the scleral extracellular matrix that is accelerated through the activation of matrix metalloproteinases [29]. Other studies suggest that the major determinants of the biomechanical properties of the optic nerve head are related to the biomechanical properties of the sclera and Lamina Cribrosa (LC) [30]. The posterior sclera and the lamina cribrosa of highly myopic eyes are significantly thinner than that of mildly myopic eyes, which results in an increase in the translaminar pressure gradient for a given IOP level [29]. Focal LC defects were found in glaucomatous eyes and highly myopic eyes without glaucoma. The increased risk of having LC defects in highly myopic eyes compared with control eyes is thought to be related to higher scleral stresses and strains [31].

It has been suggested that scleras that are ''weak'', but still within the physiologic range, will result in increased optic nerve head strains that could represent a risk factor for glaucomatous optic neuropathy [24]. Therefore, the relationship between the forces applied to the cornea and sclera and the visoelasticity of the cornea and the posterior segment are important aspects of understanding normal ocular physiology.

Recent studies suggset that the mean tensile Young's modulus of the inner optic nerve sheath is reported to be 19.8±1.6 MPa and significantly exceeds that for outer layer at 9.7±1.2 MPa; the whole sheath shows an intermediate modulus of 15.4±1.1 MPa [31]. In compression, the inner sheath was stiffer (7.9±0.5 vs 5.2±0.5 kPa) and more viscous (150.8±10.6 vs 75.6±6 kPa) than outer nerve sheath [31] suggesting that compression of the sheath would not dissipate much energy. However, stretching of the sheath as a result of stresses being transferred from the posterior sclera could lead to changes in the shape and dimensions of the LC. Posterior displacement of the LC is seen in both normal-tension and high-tension glaucoma [32]. The mehanical tensile strain in the peripapillary sclera is significantly higher than the strain in the sclera farther away from the optic nerve head [33]. In studies of individuals with unilateral glaucoma, the glaucomatous eyes have larger and more steeply curved posterior poles than the nonglaucomatous eyes indicating that a structural variation of the posterior sclera might be associated with glaucomatous optic neuropathy [32-33]. These reports further support a biomechanical relationship between the anterior cornea-limbus-scleral series biomechanical unit and the posterior sclera-optic nerve-posterior segment antomical components that are involved in maintaining ocular homeostasis.

In 2 large, randomized, double-masked trials reported in the literature, once-daily dosing of 0.02% netarsudil, a Rho kinase inhibitor, was found to be effective and well tolerated for the treatment of patients with ocular hypertension and open-angle glaucoma [34]. Rho kinase is a signaling molecule involved in regulation of pathways that control cell division and matrix metabolism during mechanotransduction [35] indicating that mechanically induced up-regulation of mechanotransduction and the resulting tissue antomical changes may play a role in the pathogenesis of ocular hypertension and glaucoma.

Conclusions

Energy storage, transmission and dissipation are important aspects of mechanical homeostasis. We recently introduced a new technique termed Vibrational Optical Coherence Tomography (VOCT) to study the anterior and posterior segment anatomic structures of pig eyes to further characterize how energy applied to the cornea and posterior segment structures is dissipated without damage to ocular tissues. In this paper we show that the large loss moduli of both the cornea and posterior segment of porcine eyes can cause dissipation of applied energy, supporting mechanical homeostasis of both the anterior and posterior segments of the eye. We conclude that a relationship exists between the anterior cornea-limbus-scleral series biomechanical unit and the sclera-optic nerve-retina and associated posterior segment complex, which effectively dissipates applied mechanical energy. The coordination of these units in dissipating applied mechanical energy protects the cornea and delicate posterior ocular structures of the eye from mechanical damage.

Author Statements

Author Contributions

Conceptualization, F.H.S., D.B. and J.P.; methodology, D.B., J.P., T.D., and M.G.-M.; formal analysis, D.B., T.D. and M.G.-M., and F.H.S.; investigation, M.G.-M. and T.D.; data curation, T.D. and M.G.-M.; writing—original draft preparation, F.H.S and D.B.; writing—review and editing, F.H.S, D.B. and J.P.; All authors have read and agreed to the published version of the manuscript.

Funding

This research wa supported in part by a grant from the J. Arch McNamara Retina Research Fund of the Wills Eye Hospital and MidAtlantic Retina

Data Availability Statement

Data are available at optovibronex.com.

Acknowledgments

The authors would like to thank Arielle Mesica for help with data collection.

Conflicts of Interest

FHS is a stockholder in OptoVibronex, LLC. and T.D. and M.G.-M. are employees

References

1. Silver FH, Gonzalez-Mercedes M, Mesica A. A rapid method to noninvasively measure the viscoelastic properties of synthetic polymers using mechanical vibrations and photonics. Photonics. 2022; 9: 925.
2. Wang Y, Cao H. Corneal and scleral biomechanics in ophthalmic diseases: an updated review. Med Novel Technol Devices. 2022; 15: 1000140.
3. Kim YC, Koo YH, Bin Hwang HB, Kang KD. The shape of posterior sclera as a biometric signature in open-angle glaucoma: an inter-eye Comparison Study. J Glaucoma. 2020; 29: 890-8.
4. Huang AS, Stenger MB, Macias BR. Gravitational influence on intraocular pressure: Implications for Spaceflight and Disease. J Glaucoma. 2019; 28: 756-64.
5. Wåhlin A, Holmlund P, Fellows AM, Malm J, Buckey JC, Eklund A. Optic nerve length before and after spaceflight. Ophthalmology. 2021; 128: 309-16.
6. Silver FH, Siperko LM, Seehra GP. Mechanobiology of force transduction in dermal tissue. Skin Res Technol. 2003; 9: 3-23.
7. Roberts TJ, Marsh RL, Weyand PG, Taylor CR. Muscular force in running turkeys: the economy of minimizing work. Science. 1997; 275: 1113-5.
8. Wilson AM, McGuigan MP, Su A, van den Bogert AJ. Horses damp the spring in their step. Nature. 2001; 414: 895-9.
9. Silver FH, Bradica G, Tria A. Elastic energy storage in human articular cartilage: estimation of the elastic modulus for type II collagen and changes associated with osteoarthritis. Matrix Biol. 2002; 21: 129-37.
10. Freeman JW, Silver FH. Elastic energy storage in unimineralized and mineralized extracellular matrices (ECMs): A comparison between molecular modeling and experimental measurements. J Theor Biol. 2004; 229: 371-81.
11. Silver FH, Bradica G, Tria A. Elastic energy storage in human articular cartilage: estimation of the elastic modulus for type II collagen and changes associated with osteoarthritis. Matrix Biol. 2002; 21: 129-37.
12. Horvath I, Foran DJ, Silver FH. Energy analysis of flow induced harmonic motion in blood vessel walls. Cardiovasc Eng. 2005; 5: 21-8.
13. Kaufman PL, Lütjen Drecoll E, Croft MA. Presbyopia and glaucoma: two diseases, one pathophysiology? The 2017 Friedenwald lecture. Invest Ophthalmol Vis Sci. 2019; 60: 1801-12.
14. Sasakai N, Odajima S. Elongation mechanism of collagen fibrils and force–strain relationships of tendon at each level of structural hierarchy. J Biomech. 1996; 9: 1131-6.
15. Sasaki N, Odajima S. Stress–strain curve and Young's modulus of a collagen molecule as determined by the X-ray diffraction technique. J Biomech. 1996; 29: 655-8.
16. Mosler E, Folkhard W, Knörzer E, Nemetschek-Gansler H, Nemetschek TH, Koch MH. Stress-induced molecular arrangement in tendon collagen. J Mol Biol. 1985; 182: 589-96.
17. Silver FH, Freeman JW, Seehra GP. Collagen self-assembly and the development of tendon mechanical properties. J Biomech. 2003; 36: 1529-53.
18. Silver FH, Shah RG. Mechanical analysis of multi-component tissues. World J Mech. 2017; 07: 121-32.
19. Silver FH, Kelkar N, Deshmukh T. Molecular basis for mechanical properties of ECMs: proposed role of fibrillar collagen and proteoglycans in tissue biomechanics. Biomolecules. 2021; 11: 1018.
20. Shah RG, Silver FH. Viscoelastic behavior of tissues and implant materials: estimation of the elastic modulus and viscous contribution using optical coherence tomography and vibrational analysis. J Biomed Tech Res. 2017; 3: 105-9.
21. Crespo MA, Jimenez HJ, Deshmukh T, Pulido JS, Saad AS, Silver FH, et al. In vivo determination of the human corneal elastic modulus using vibrational optical coherence tomography. Transl Vis Sci Technol. 2022; 11: 11.
22. Silver FH, Deshmukh T, Kelkar N, Ritter K, Ryan N, Nadiminti H. The "virtual biopsy" of cancerous lesions in 3D: non-invasive differentiation between melanoma and other lesions using vibrational optical coherence tomography. Dermatopathology (Basel). 2021; 8: 539-51.
23. Silver FH, Desmukh T, Gonzalez-Mercedes M. Use of Vibrational Optical Coherence Tomography to noninvasively Differentiate between Benign fibrotic Tissue and Fibrosis Associated with Melanoma, 21st-century pathology. 2023; 3: 139.
24. Eilaghi A, Flanagan JG, Simmons CA, Ethier CR. Effects of scleral stiffness properties on optic nerve head biomechanics. Ann Biomed Eng. 2010; 38: 1586-92.
25. Dastiridou AI, Ginis HS, De Brouwere D, Tsilimbaris MK, Pallikaris IG. Ocular Rigidity, Ocular Pulse Amplitude, and Pulsatile Ocular Blood Flow: The Effect of Intraocular Pressure. Invest Ophthalmol Vis Sci. 2009; 50: 5718–5722.
26. Jonas JB, Wang N. Cerebrospinal fluid pressure and glaucoma. J Ophthalmic Vis Res. 2013; 8: 257-63.
27. Fazio MA, Grytz R, Morris JS, Bruno L, Gardiner SK, Girkin CA et al. Age-related changes in human peripapillary scleral strain. Biomech Model Mechanobiol. 2014; 13: 551-63.
28. Jiang B, Shi CS. Dynamic changes of periostin and collagen I in the sclera during progressive myopia in Guinea pigs. Arq Bras Oftalmol. 2020; 83: 190-5.
29. Guggenheim JA, McBrien NA. Form-deprevation myopia induces activation of sclera matrix metalloproteinase-2 in tree shew. Invest Ophthalmol Vis Sci. 1996; 37: 1380-95.
30. Voorhees AP, Hua Y, Brazile BL, Wang B, Waxman S, Schuman JS, et al. So-called lamina cribrosa defects may mitigate IOP-induced neural tissue insult. Invest Ophthalmol Vis Sci. 2020; 61: 15.
31. Miki A, Ikuno Y, Asai T, Usui S, Nishida K. Defects of the lamina cribrosa in high myopia and glaucoma. PLOS ONE. 2015; 10: e0137909.
32. Shin A, Park J, Le A, Poukens V, Demer JL. Bilaminar mechanics of the human optic nerve sheath. Curr Eye Res. 2020; 45: 854-63.
33. Li L, Bian A, Cheng G, Zhou Q. Posterior displacement of the lamina cribrosa in normal-tension and high-tension glaucoma. Acta Ophthalmol. 2016; 94: e492-500.

34. Fazio MA, Grytz R, Morris JS, Bruno L, Gardiner SK, Girkin CA, et al. Age-related changes in human peripapillary scleral strain. Biomech Model Mechanobiol. 2014; 13: 551-63.

35. Serle JB, Katz LJ, McLaurin E, Heah T, Ramirez-Davis N, Usner DW, et al. Two Phase 3 clinical trials comparing the safety and efficacy of Netarsudil to timolol in patients with elevated intraocular pressure: rho kinase elevated IOP treatment Trial 1 and 2 (ROCKET-1 and ROCKET-2). Am J Ophthalmol. 2018; 186: 116-27.

36. Ohashi K, Fujiwara S, Mizuno KJ. Roles of the cytoskeleton, cell adhesion and rho signalling in mechanosensing and mechanotransduction. J Biochem. 2017; 161: 245-54.